Modelling alluvial channel dynamics in a river reach dominated by alternate bars

N. Rüther
Department of Hydraulic and Environmental Engineering, Norwegian University of Science and Technology, S.P. Andersens veg 5, 7491 Trondheim

M. Guerrero & A. Lamberti
Hydraulic Laboratory – DISTART Department, Bologna University, via Terracini, 40131 Bologna, Italy

ABSTRACT: A three dimensional CFD model was used to compute the flow, suspended sediment concentrations and the corresponding bed change over time in a natural river reach of 4km length. The river reach is a part of the river Po near Boretto, Italy and its river bed is dominated by alternate bar development. The results of the model are compared to data from a detailed acoustic Doppler and backscattering survey carried out in the years of 2005, 2006 and 2007 of Bologna University, Italy. The CFD model solved the Reynolds-averaged Navier-Stokes (RANS) equations in three dimensions to compute the water flow and was fully coupled with a sediment transport routine to predict the suspended sediment concentrations and the transient bed deformation. The bed level changes were calculated by solving the continuity equation of the sediment concentration at the bed. In addition to the 3D simulation, the same reach was modeled with a 2D hydrodynamic code with a coupled sediment transport routine and an adaption to three dimensional flow characteristics (quasi 3D (Q3D)). The goal of the study was to investigate the 3D and 2D numerical results for a better understanding of fluvial processes at different scales and to identify uncertainties in the results of the long term 2D simulations. The 3D approach uses a universal method for the calculation of the secondary flow that appears to be important in the observed grain size sorting and alternate bars development. The outcome of the study will improve the quality of long term prediction of a 2D simulation, which is important e.g. navigation channel maintenance.

Keywords: Fluvial sediment transport, Sediment transport modelling, CFD, Depth averaged, River Po

1 INTRODUCTION

Nowadays commercial numerical models are available, for instance Delft Hydraulics and DHI software, which simulate the two-dimensional (2D) shallow water equation for the flow coupled which a sediment transport module to simulate fluvial processes and river bed evolution. These numerical tools are designed to simulate river branches for some tenth of kilometers length over a longer period of time. These kinds of simulations give insight in long term impact of e.g. climate change on river channels, fluvial navigation, bank stability and reservoir capacities. This advantage comes along with the disadvantage that certain physical processes have to be modeled with approximations. Oversimplifications regarding shear process, secondary flow and sediment transport leads to the need of verifying the results thoroughly. It is recommended to calibrate the model accurately for at least a steady situation, us-

ing measurements of velocity field, sediment transport and channel morphology. Another alternative could be, to use the results of a fully three dimensional (3D) flow and sediment computation to calibrate the 2D model. This approach is much more cost effective and would save time, too. The current investigation tries to evaluate this possibility by using a 3D numerical model and comparing the results to measurements and the results of the 2D numerical model. Therefore is the present study assessing and pointing out further needs in order to be successful in providing calibration data for a 2D model by using a 3D numerical model.

2 FIELD DATA

Two campaigns were carried out on the Po river, the major river in Italy. Its main channel is 650 km long, and its 71000 km² catchment includes most of the Italian Alpine slopes, the Po plain

(Pianura Padana) and the Emilian slopes of the Apennine mountains. The average and historical maximum discharges are about 1500 and 12000 m^3/s, and the transport of bed sediments is estimated from past delta extension and subsidence as having decreased in the last century from 10 to 5 10^{6}m^3/year (Cati, 1981). The monitored reach is near Boretto, 216 km from the Adriatic sea, where the catchment area is 55200 km^2; the alluvial bed is composed of well sorted coarse sand with mean size near 0.5 mm and sorting 1.2 phi. Water flows towards south east, with a mean slope variable around 0.15 m/km.

Figure 1 shows the multibeam bathymetry of the 2D and 3D modeled reach, it is 5.2 km long and 250 m wide and includes a straight upstream reach, alternate bar dominated, and the two consecutive bends with the intermediate flex.
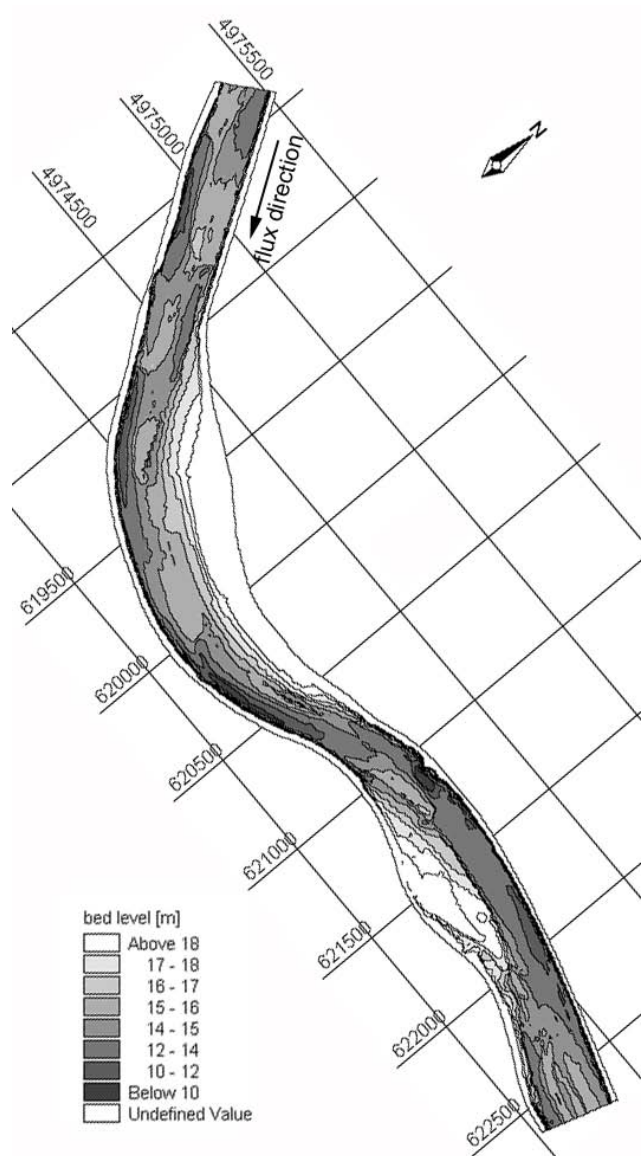

Figure 1 Multibeam bathymetry

The first campaign was carried out on 7 and 8 Nov 2006, the second on 8,9 and 10 May 2007; in both cases low flow conditions were surveyed inside a two dry years period (May 2005–May 2007). The May survey was carried out during a moderate flow; the mean level during the period at Boretto was -1.40 m with a standard deviation of 0.35 m; the stage was regularly falling at a rate of 0.5 m/day. The assessed mean flow was 974 m^3/s.

Two Teledyne RDI aDcps were used, working at 600 and 1200 kHz, placed side by side down looking on a moving vessel, insonified the same water column. Echoes of two different frequencies were continuously recorded together with velocity profiles. A dynamic survey was carried out over the whole reach, following longitudinal and transversal transects. In order to reduce the non stationary effects on the surveyed data each campaign takes no more than 3 days.

The available data consist in profiles, cross sections and depth averaged maps of velocity and suspended sediment fields, furthermore the bathymetry (fig. 1) was simultaneously surveyed with a Kongsberg 300 kHz multibeam.

The shear velocity assessed by the logarithmic fitting method of aDcp surveyed profiles (Rennie and Church, 2007), the deviation between the upper and the lower part of velocity aDcp profile that is in relation with helical flow (Yalin and da Silva, 2001), and the concentration profiles derived from 2 aDcp echoes profiles using the multi frequency method (Guerrero and Lamberti, 2008), are particularly useful for steady calibration of velocity and sediment transport fields.

3 NUMERICAL METHODS

3.1 *2D numerical model*

The 2D, shallow water approximation, code was the MIKE21C by Danish Hydraulic Institute. The model solves two-dimensional Navier-Stokes equations on a curvilinear grid using the finite difference scheme. A wet and dry algorithm allows water stage to change significantly during simulation, except near the boundary condition locations. Bed roughness can be defined as a constant, as a map or variable with depth in order to account of bed forms shear.

Hydrodynamics vertical dimension features, i.e. logarithmic profiles and helical flow, are taken into account both on the two-dimensional convective-diffusive equation and on bed load. The 2D convective-diffusive equation is derived from the Galappatti (Galappatti, 1983) approach for quasi steady concentration profile, and assuming the equilibrium of concentration near the bed. In that way the concentration time and spatial derivatives are multiplied by coefficients coming from velocity and concentration profile vertical integrations, but that can be also tuned in agreement with field

evidences. The bed load is diverted from velocity direction depending on bed slope and channel curvature as described by first order model of Kalkwijk (Kalkwijk et al. 1987), that can be calibrated in agreement with field evidences. These features make the model quasi 3D, but introduce some parameters that need to be accurately calibrated.

In agreement with mentioned schemes, the sediment continuity and convective-diffusive equations are solved in a quasi steady approach also with the aim to speed up long term morphodynamic simulations. For this reason the model is particularly fitted for long term and slowly variable morphodynamics simulations.

3.2 *3D numerical model*

The numerical model SSIIM is used in this study (Olsen 2007). The program uses a non-orthogonal unstructured grid. In the plan view, the grid follows the river. The unstructured nature of the grid makes it possible to use a varying number of grid cells in all three spatial directions, according to the water depth and the area covered by water. The number of vertical cell varies from 1 at the sides to 21 in the deepest parts of the domain. The grid cell size in the horizontal directions was approximately 5.0 × 3.0 m.

Zero gradient boundary conditions were used for all variables at the outflow boundary, while velocities were specified at the inflow boundary (Dirichlet boundary condition). Wall laws introduced by Schlichting (1979) were used for the side walls and the bed. The bed roughness can be given as either a user input or computed by the model as a function of the bed sediment distribution. In the present case, it was set to a constant value. The water surface was initially computed with a 1D backwater approach and an overall roughness value, and compared to the measured water surface. During the simulation the water surface was kept constant. This assumption was valid since the simulation was steady.

The flow field for the three-dimensional geometry was determined by solving the continuity equation and the Reynolds averaged Navier–Stokes equations. The control volume method was used for discretization (Olsen, 2007) and the convective terms in the Navier–Stokes equations were solved by a first- or second-order upwind scheme. The pressure field was computed with the SIMPLE method (Patankar, 1980). SIMPLE stands for "Semi-Implicit Method for Pressure-Linked Equations" and solves the unknown pressure field with an iterative process based on the continuity defect. The Rhie and Chow interpolation (Rhie & Chow, 1983) was applied to compute the velocities and

fluxes at the cell surfaces. The standard two-equation k–ε turbulence closure (Rodi, 1980) was used to compute the turbulent viscosity and diffusivity. The suspended sediment transport was calculated by solving the transient convection-diffusion equation for sediment concentration. To define the boundary conditions for the bed load and suspended sediment concentration, van Rijn's (1984a, b) were applied to the cells adjacent to the bed.

4 RESULTS AND DISCUSSION

4.1 *Results of the 2D numerical model*

A first step for an accurate morphodynamic calibration is the comparison between simulated and surveyed velocity and sediment transport fields. With that aim the MIKE21C numerical model is applied to the case study of May 2007 survey, simulating the time averaged condition over the surveyed period.

Figure 1 shows the implemented bathymetry. On average the computation curvilinear grid has a 10 meters side square cell. The downstream condition on water level and the upstream one on discharge, come respectively from water stage measurement and aDcp velocity profile integration over 10 cross sections. The bed roughness derived from logarithmic fitting of aDcp profiles is imposed as a map or as spatially averaged value of Chezy parameter all over the study area, being negligible the deference on following results.

In general must be said that there's a strong agreement between simulated and measured water depths and levels, as a consequence the model accurately reproduces the depth-velocity correlation changing along the reach from weakly positive/nearly negative (i.e.: high velocity approaching low depths) at upstream bar dominated sub-reach to clearly positive (i.e.: high velocity at high depths) in the downstream bended sub-reach.

In figure 2 the depth averaged velocity field resulting from 2D shallow water simulation can be compared with depth averaged velocity magnitude of aDcp profiles. The two velocity maps are very similar in particular the upstream straight sub-reach appears to be dominated by alternate bars that give rise to a typical alternating pattern of low and high velocity values. The major velocities both for 2D simulated and surveyed fields are downstream shifted with respect to greater depth, i.e. the bar through, that giving evidence about the flux contraction taking place over the bar toss side. The more downstream bar protrudes into the first bend, splitting and moving downstream, with respect to bend apex, the location of maximal ve-

locity. In fact the highest surveyed velocities appear both near the apex, at low depth over the bar ridge, and at following flex where the scour in figure 1 indicates the flux impact zone. The simulated velocity field shows high values, above 1 m/s, all over the outer side of upstream bend, where as the measured values show slightly lower ones. The downstream bend shows a good agreement between simulated and surveyed velocity, perhaps except the area following the flex where lower values appear in the surveyed map due to the bridge pear that is not represented in the model.
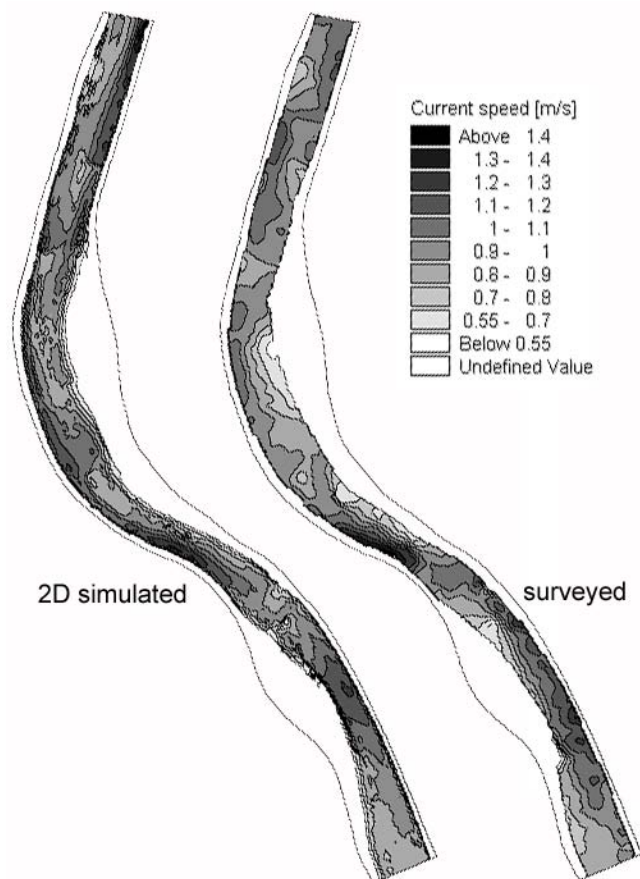
Figure 2 Velocity fields comparison.

The first order model of Kalkwijk et al. 1987, for bed load deviation, is calibrated on field evidence concerning the deviation between upper and bottom part of velocity aDcp profiles. In figure 3 the simulated bed load deviation referred to depth averaged velocity can be compared with measured deviation. Theoretically speaking, the two angles are not the same even if the measured surveyed map of figure 3 shows the halved value of up-bottom deviation, in that way accounting of two angles different references and assuming an almost symmetric secondary velocity profile. Notwithstanding the mentioned differences, the two deviations are indications of the same helical flow and secondary flow processes. As a consequence the two maps of figure 3 show similar patterns and values. In particular the model represents the same

wave length, of about 1 km, as the prototype of the consecutive deviation changing sign all over the upstream straight sub-reach, where flow is diverted from left to right and vice versa by alternate bars. Follow the bended sub-reach where the deviation is dominated by river curvature. As for velocity field (figure 2) the model only roughly approximates the process that take place between upstream bend apex and following flex where alternate bar field protrudes into the following bend and the two elsewhere well observable behaviors, alternate bar and river curvature dominated, are blended together. In fact the surveyed map in that area shows a clear switch from positive to negative deviation that appear to be dampened by the model.
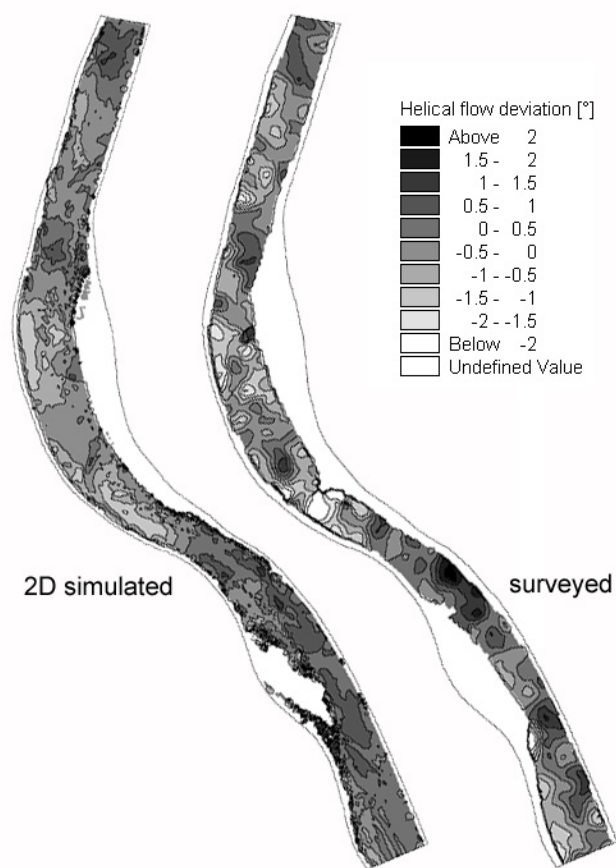

Figure 3 2D simulated and measured helical flow.

The 2D steady concentration field is simulated starting from a zero concentration initial condition and assuming the bed equilibrium at upstream boundary during the necessary time to get a steady configuration all over the computational domain. The bed material is represented with the mean grain size from bed samplers and van Rijn formulations are applied both for bed and suspended load. In figure 4, the resulting concentration field can be compared with surveyed one, being both depth averaged values, but taking in mind that the aDcp measurements are lacking the near bed part of profiles where sediment transport is usually confined. Even if the model catches the surveyed

patters and the domain mean value of simulated and surveyed maps are fairly near, a clear difference appears in the amplitude of maximal and floor values. In fact the measured map show higher peaks of concentration over a lower base. The evidences concerning also the infield observed grain size sorting allover surveyed reach, suggest a graded model would better approximate the measured concentration field by simulating higher maximal concentration of finer material above a lower base of coarse sediments.
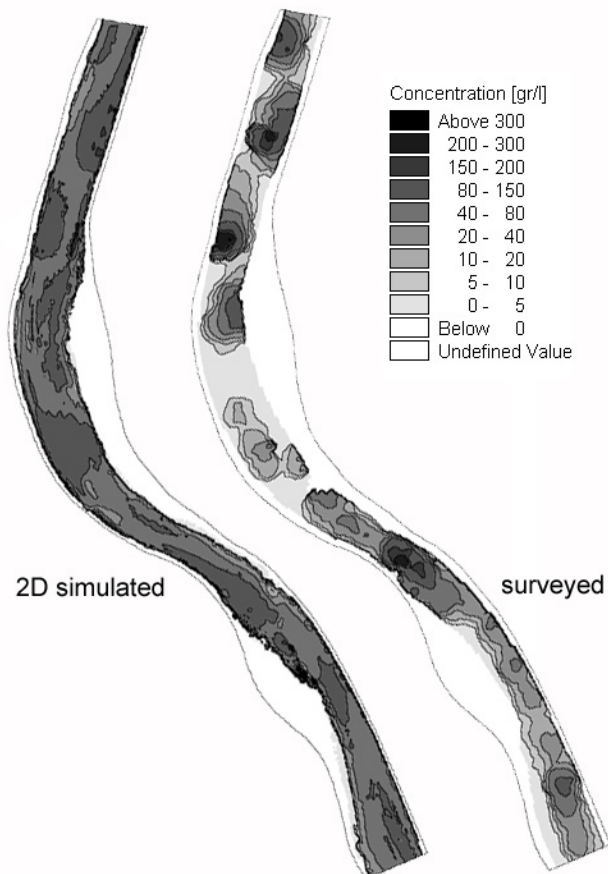

Figure 4 Depth averaged concentration.

4.2 *Results of the 3D numerical model*

The 3D computed velocities were depth averaged and compared to the measurements. The results are depicted in Figure 5. The range of the depth averaged velocities is displayed from 0.1 to 1.4 m/s. The overall agreement is very satisfying. The river reach can be divided into three subsections: The upper part with the alternate bar formation, the middle part with the bend flow and the downstream part with the contracted, accelerated flow. The flow pattern in upstream part of the river reach reflects the pattern of the alternate bar formation. The velocity maximum shifts from left to right each time the geometry changes. In the middle part the flow is dominated by the bend flow. In the upstream part of the bend, one can see that the 3D model clearly overestimates the mag-

nitude of the depth average velocity. At the end of the bend where the flow is accelerated, the model results are in good agreement with the measurement. The maximum of the velocity is at the outside of the bend. Similar good results can be observed both, in the subsequent cross over and the bend to the other side. Both, location of maximum velocity and distribution of velocity are matching very well with the measurements.
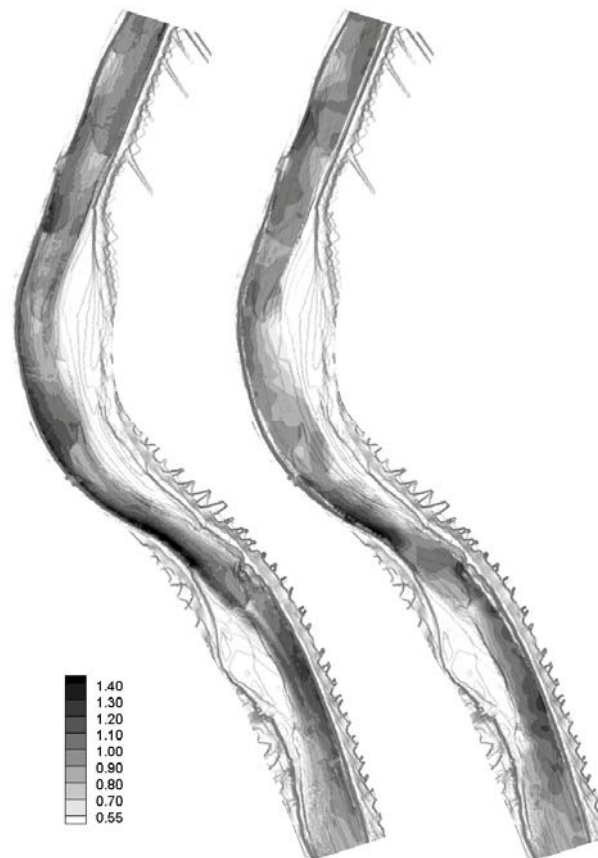

Figure 5 Depth averaged velocities from 3D simulation compared to measurements.

Figure 6 shows the calculated deviation of the velocity vectors at the surface and at the bottom and the comparison to the measurements. The right plot shows the measured values. When comparing the data with simulated results one has to be aware of the fact that the measurements were taken 0.9 m below the surface and 0.5 m from the bottom. Therefore one can explain the consistent deviation in magnitude in comparison to the simulation. However, the figure indicates that the locations of the deviation are matching. This is due the fact that deviation is clearly dominated by the bottom topography. This feature seems to be important since the bed load transport is following the direction of the near bed flow. .
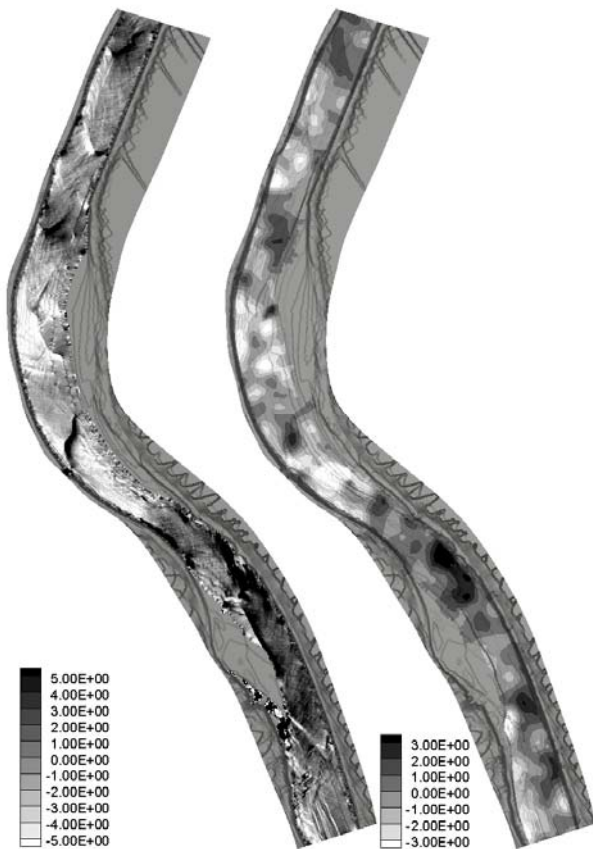
Figure 6 3D calculated helical flow compared to the measured values

Figure 7 displays the comparison of the bed shear stress between the calculated values on left side and the measured values to the right side. The values range from 1.0 to 7.0 N/m^2. The pattern of the shear stress is strongly linked to the topography. In the upstream part of the river reach the peaks of bottom shears stress are following the heads of the alternate bars. Entering the bend, the location of the maximum bed shear stress is pushed to the outside to find its maximum on the top of the prevailing bar. This is not observed in the measurements. Here the numerical model strongly overestimates the bottom shear stress. Throughout the bend and downstream the bend the shear stress matches again very well.

Figure 8 shows the calculated and measured concentration of suspended sediments. The measured values are displayed as depth averaged, whereas the calculated values are extracted from 0.15 x the maximum depth in that water column. One can see that patter matches in a very well agreement. It is linearly connected to the shear stress pattern. Again one can observe that in the beginning of the upstream bend the concentration are overestimated. This might be due to the large alternate bar traveling through the bend.

4.3 Discussion

The comparison in the previous chapter shows that there can be a significant difference in the result of the simulation with different numerical methods. This is for example in case of the calculated deviation of the surface to bottom velocity vectors. Even though the 2D approach is considering the bed topography in a certain way, it seems that in the reach of the bend flow the model is overestimating the pure helical flow effect due to bed flow. Instead the bed topography is dominating the deviation of the flow.
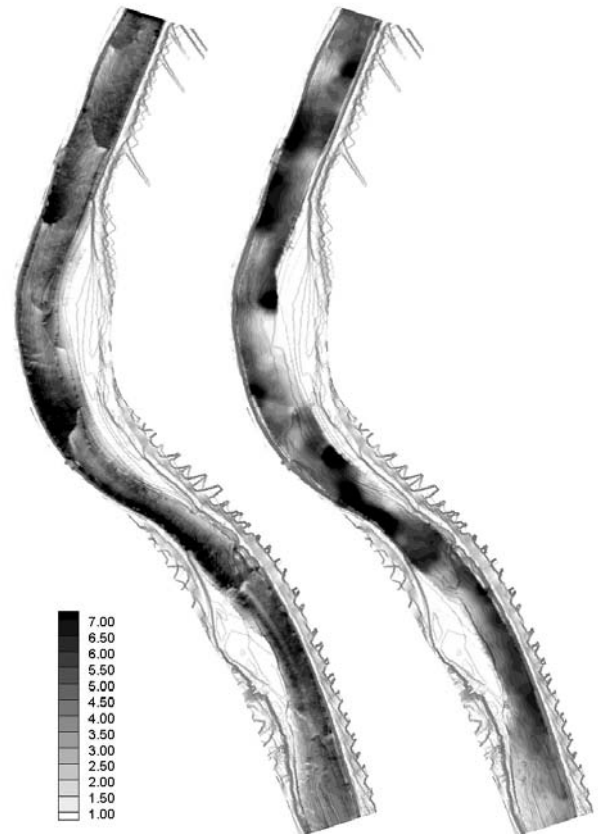

Figure 7 3D calculated shear stress distribution at the river bed

At the same time one can state that for some computations the 2D and the 3D model give the same results. Considering e.g. the depth averaged velocity both models seem to have the same problem to calculate the measured values. Both models are overestimating the magnitude in the upstream part of the bend. This deviation could be referred to unsteadiness during the measurements which are not representing the time averaged numerical results. One possible error could have been if there was a change in the gradient of the water surface which lead to lower velocities and lower shear stress as calculated. This scenario was calculated by using a water surface level where the gradients differ with respect to the longitudinal coordinate. Unfortunately this did not show improvement of the results.
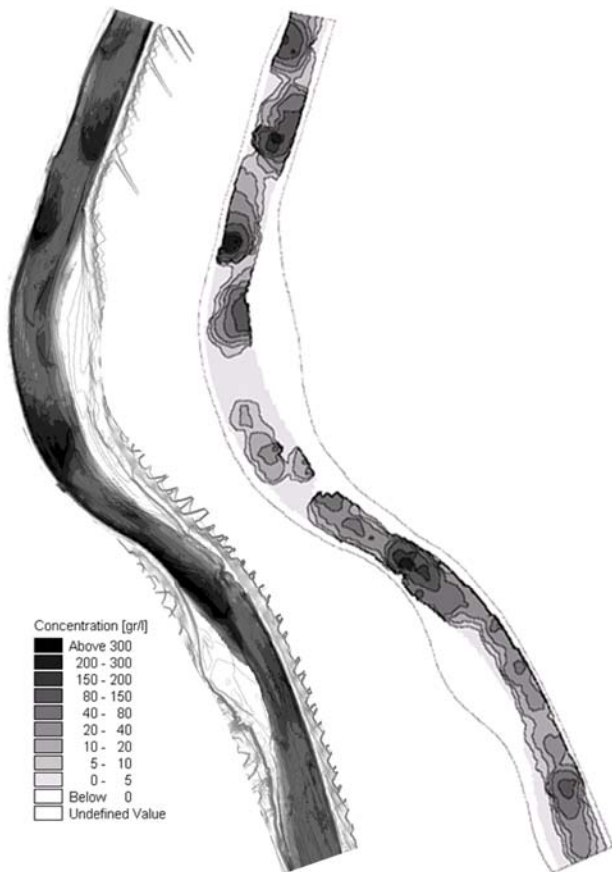
Figure 8 Comparison of calculated (at 0.15 x water depth) and the measured sediment concentrations (depth averaged)

5 CONCLUSION AND RECOMMENDATION

In the present study the characteristic flow features and the average sediment transport capacity have been calculated with a 2D and 3D numerical model. The results of the calculation have been compared to measurements taken in the River Po. The comparison between the 3D and the 2D numerical results show that the different numerical methods are facing the same problems when looking in the first part of the upstream bend. Both numerical models overestimate the velocity and the sediment concentrations at this location. Besides that, one can state that the results of the 3D numerical model are slightly superior compared to the 2D calculated results. Especially when looking at the deviation of the velocity vectors at the surface and at the bed. Consequently are the results for the computation of the sediment concentration better, too.

Whether the results from the 3D calculations are good enough to perform a calibration instead of using the measured values can't be answered finally. Further investigations and comparison are necessary before a final conclusion can be drawn.

REFERENCES

Cati L., 1981. Idrografia e Idrologia del Po. Ufficio Idrografico del Po.

Galappatti R., 1983. A depth-integrated model for suspended transport. Communications on Hydraulics 83-7. Dept. of Civil Engineering, Delft Univ. of Technology.

Guerrero, M. & A. Lamberti. Field measurements of suspended sediment transport with acoustic multi frequencies technique, River Flow 2008, Cesme-Izmir Turkey, 3-5 September 2008, (3) 2335-2341, ISBN 978-605-60136-3-8.

Kalkwijk J.P.T., Booij R., 1986. Adaptation of secondary flow to nearly horizontal flow. Journal of Hydraulic Research, 24(1), 19-37.

Olsen, N.R.B., 2007. A Three-dimensional Numerical Model for Simulation of Sediment Movements in Water Intakes with Multiblock Option. Norwegian University of Science and Technology, Trondheim

Rennie C.D., M. Church. ADCP shear stress and bed load transport in a large wandering gravel-bed river. Proceedings of 32° Congress of IAHR, July 1-6, 2007, Venice.

Rodi, W., 1980. Turbulence Models and Their Application in Hydraulics. A. A. Balkema, Rotterdam

Rhie, C.M. & Chow, C.L., 1983. Numerical study of the turbulent flow past an airfoil with trailing edge separation. Am. Inst. Aeronaut. Astronaut. 21 (11), 1523–1532

Schlichting, H. 1979 Boundary Layer Theory, McGraw-Hill

van Rijn L.C., 1984a. Part I: Bed load transport, Journal of Hydraulic Engineering, 110(10), 1431-1456.

van Rijn L.C., 1984b. Part II: Suspended load transport, Journal of Hydraulic Engineering, 110(11), 1613-1641.

Yalin M. S., da Silva A.M.F., 2001. Fluvial Processes. IAHR Monograph.